A Two-Dimensional Finite Element Formulation of the Perfectly Matched Layer

Anastasis C. Polycarpou, *Student Member, IEEE*, Michael R. Lyons, *Student Member, IEEE*, and Constantine A. Balanis, *Fellow, IEEE*

Abstract— **A perfectly matched layer (PML) is implemented using the finite element method (FEM) to successfully terminate the output port of a parallel-plate waveguide operating over a wide range of frequencies. The PML layer is modeled as a nonphysical anisotropic lossy material backed with a perfect electric conductor (PEC). Numerical results showing the reflection coefficient as a function of frequency, for both TEM and TM_1 propagation modes, demonstrate the effectiveness and accuracy of the PML concept as applied in the context of the FEM.**

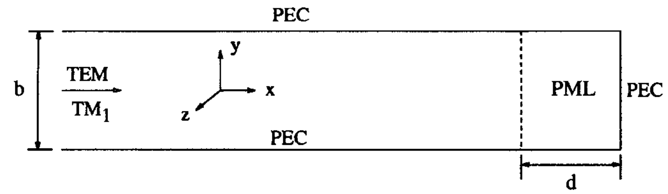

Fig. 1. Parallel-plate waveguide terminated with a PML absorbing boundary condition.

I. Introduction

The FINITE element method (FEM) is a very versatile and powerful numerical technique for solving electromagnetic propagation problems. The capability to accurately model geometrical and material complexities provides the method with a great advantage over other numerical techniques such as the method of moments (MoM) or the finite-difference time-domain (FDTD) method. However, the FEM faces a large number of challenges, such as an accurate and numerically efficient termination of the finite element mesh that would still simulate undisturbed wave propagation in a given medium.

The recently developed perfectly matched layer (PML) [1], which was mainly implemented in the context of the finite-difference time-domain (FDTD) technique [2]–[4], resulted in a significant improvement over other previously used absorbing boundary conditions (ABC's) in reducing reflections due to mesh truncation. The required computational resources have also significantly declined since the PML interface can be placed much closer to a physical structure compared to other well known ABC's.

Although the PML concept had an incredible impact in modeling electromagnetic wave propagation problems using the FDTD method, the idea has not yet been adopted widely in modeling similar problems using the FEM. An FEM implementation of the PML concept, as applied to scattering problems, was recently published by Pekel and Mittra [5]. More recently, a paper written by Sacks *et al.* [6] introduced the PML absorbing boundary condition in calculating far-field radiation patterns of a single dipole. However, none of the above quantifies the numerical error introduced due to terminating the finite element mesh with a PML region.

Manuscript received April 4, 1996. This work was supported by the U.S. Army Research Office under grant DAAL03-92-G-0262.

The authors are with the Department of Electrical Engineering, Telecommunications Research Center, Arizona State University, Tempe, AZ 85287-7206 USA.

Publisher Item Identifier S 1051-8207(96)06520-8.

This letter formulates the PML in the context of the FEM as applied to two-dimensional (2-D) waveguide structures. The main idea is to model the PML medium as a uniaxial anisotropic lossy material. According to Berenger [1], the only restriction on the properties of the material is that the condition $\sigma/\epsilon_d = \sigma^*/\mu_d$ is satisfied, where σ is the electric conductivity, σ^* is the magnetic conductivity, and ϵ_d and μ_d are the permittivity and permeability of the PML region, respectively.

A parallel-plate waveguide, shown in Fig. 1, is excited with either a TEM or TM_1 mode. The reflection error due to a PML termination is quantified by calculating the reflection coefficient of an empty waveguide using various mesh discretizations. Obtained results for the reflection coefficient illustrate the effectiveness of the PML medium using the FEM as compared to previously published data using the FDTD method [4], [7].

II. Theory

The electric field vector equation given by

$$\nabla \times (\bar{\bar{\mu}}_r^{-1} \cdot \nabla \times \mathbf{E}) - k_o^2 \bar{\bar{\epsilon}}_r \mathbf{E} = 0 \tag{1}$$

is broken down into two different partial differential equations: one describing the longitudinal electric fields (TM_1 mode) and the other describing the transverse electric fields (TEM mode). The permittivity and permeability tensors, $\bar{\bar{\epsilon}}_r$ and $\bar{\bar{\mu}}_r$, are 2×2 block matrices and, as a result, the two equations are completely decoupled from each other. In addition, the fields are invariant in the longitudinal (z-axis) direction. The resulting decoupled integral equations are the following:

$$\iint_\Omega [(\nabla_t \times \mathbf{E}_t)\, \tilde{\tilde{\mu}}_r (\nabla_t \times \mathbf{E}_t)^* - k_o^2 \mathbf{E}_t\, \bar{\bar{\epsilon}}_r \mathbf{E}_t^*]\, d\Omega = 0 \tag{2}$$

$$\iint_\Omega [(\nabla_t E_z)\, \tilde{\tilde{\mu}}_r (\nabla_t E_z^*) - k_o^2 E_z\, \bar{\bar{\epsilon}}_r E_z^*]\, d\Omega = 0 \tag{3}$$

where ∇_t is the transverse del operator, $\mathbf{E}_t$ is the transverse component of the electric field, and E_z is the longitudinal component of the electric field. The tensor $\tilde{\tilde{\mu}}_r$, referred to as the relative pseudo-permeability, has also been introduced and is defined as

$$\tilde{\tilde{\mu}}_r = \begin{bmatrix} \mu_{yy}^{inv} & -\mu_{yx}^{inv} & 0 \\ -\mu_{xy}^{inv} & \mu_{xx}^{inv} & 0 \\ 0 & 0 & \mu_{zz}^{inv} \end{bmatrix}. \quad (4)$$

The transverse fields, $\mathbf{E}_t$, are expanded in terms of linear edge-based triangular elements, whereas the longitudinal fields, E_z, are expanded in terms of linear nodal-based triangular elements.

A parallel-plate waveguide, shown in Fig. 1, was chosen in this letter to investigate and quantify the reflection error due to the PML termination. The main reason for selecting such a geometry is because 2-D problems are usually more intuitive and informative. The parallel-plate waveguide is excited either with a TEM mode or a TM_1 mode, where the latter exhibits a cutoff frequency at $f = c/2b$. The mixed boundary condition at the input port assumes that only the dominant mode is propagating inside the waveguide, whereas the output port is terminated with a PML region of depth d. The PML region is subsequently subdivided into N layers, each defined with a different electric and magnetic conductivity. The corresponding conductivities are given by

$$\sigma(x) = \frac{(m+1)\epsilon_o\epsilon_r c}{2d} \ln\left(\frac{1}{R}\right)\left(\frac{x-x_o}{d}\right)^m \quad (5)$$

$$\sigma^*(x) = \frac{(m+1)\mu_o\mu_r c}{2d} \ln\left(\frac{1}{R}\right)\left(\frac{x-x_o}{d}\right)^m \quad (6)$$

where m is the order of the spatial polynomial, R is the desired reflection coefficient at normal incidence, and x_o is the position of the PML interface (assuming that the interface lies on the yz-plane). The relative permittivity and permeability tensors of a PML layer that is oriented such that it maximizes absorption of waves traveling in the x-direction are given by

$$\bar{\bar{\epsilon}}_r^p = \epsilon_r \begin{bmatrix} \frac{1}{1 - j\frac{\sigma}{\omega\epsilon_r\epsilon_o}} & 0 & 0 \\ 0 & 1 - j\frac{\sigma}{\omega\epsilon_r\epsilon_o} & 0 \\ 0 & 0 & 1 - j\frac{\sigma}{\omega\epsilon_r\epsilon_o} \end{bmatrix} \quad (7)$$

and

$$\bar{\bar{\mu}}_r^p = \mu_r \begin{bmatrix} \frac{1}{1 - j\frac{\sigma^*}{\omega\mu_r\mu_o}} & 0 & 0 \\ 0 & 1 - j\frac{\sigma^*}{\omega\mu_r\mu_o} & 0 \\ 0 & 0 & 1 - \frac{\sigma^*}{\omega\mu_r\mu_o} \end{bmatrix} \quad (8)$$

respectively. The tensor formulation described above naturally causes a rapid decay of electromagnetic fields traveling in the x-direction. In addition, it is important to mention here that although the effectiveness of the PML medium is independent of the incident angle θ, terminating it with a perfect electric conductor results in an angle-dependent reflection coefficient of the form [1]

$$R(\theta) = R(0)^{\cos(\theta)}. \quad (9)$$

TABLE I
MESH INFORMATION FOR THE CASE WHERE $N = 10$ AND $d = 20$ mm

Mesh #	# of Triangles	# of Edges	# of Nodes
1	5,175	7,872	2,698
2	11,339	17,169	5,831
3	22,571	34,084	11,514

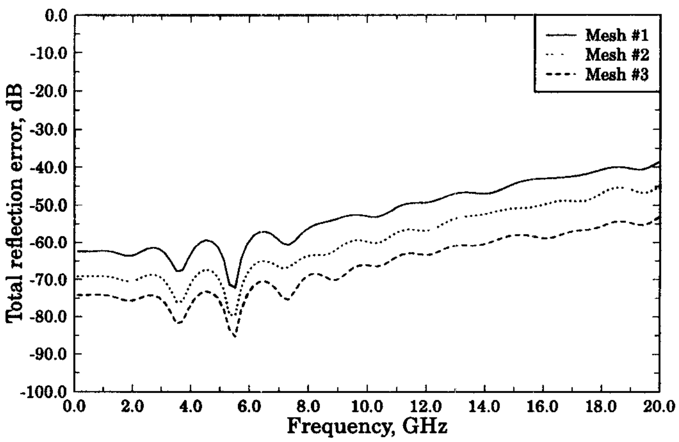

Fig. 2. Reflection error due to the PML termination for various finite element discretizations—$N = 10$, $d = 20$ mm, $m = 2$, $R = 1.0E-4$, TEM mode.

III. RESULTS

The first case considered was an empty parallel-plate waveguide with wall separation of $b = 40$ mm. The output port was terminated with a ten-layer PML medium of total depth equal to 20 mm. The waveguide was excited with two different modes: a TEM mode, which exhibits no cutoff frequency, and a TM_1 mode with $f_c = 3.75$ GHz. Three different discretizations (see Table I) were considered. The corresponding reflection coefficient [20 log (S_{11})] as a function of frequency, for both cases of excitation, is illustrated in Figs. 2 and 3. It is interesting to see that at lower frequencies the reflection coefficient reaches levels as low as −75 dB with the trend of reducing it even further by additional refined discretization. In Fig. 3, it is shown that the reflection coefficient increases rapidly at frequencies close to cutoff. This is something expected, however, since close to cutoff the wave propagates very slowly, whereas at cutoff the wave does not propagate at all. It is also important to emphasize that the reflection coefficient shown in Figs. 2 and 3 is a combined effect due to a reflection from the PML medium as well as the finite element discretization. The latter explains the increasing slope of the reflection coefficient versus frequency (note that the discretization error is of order h^2 where h is the maximum triangle edge).

The PML medium was also parameterized by plotting the reflection coefficient as a function of frequency for different values of the spatial polynomial order as in (5) and (6). Fig. 4 demonstrates that by increasing the order of the polynomial,

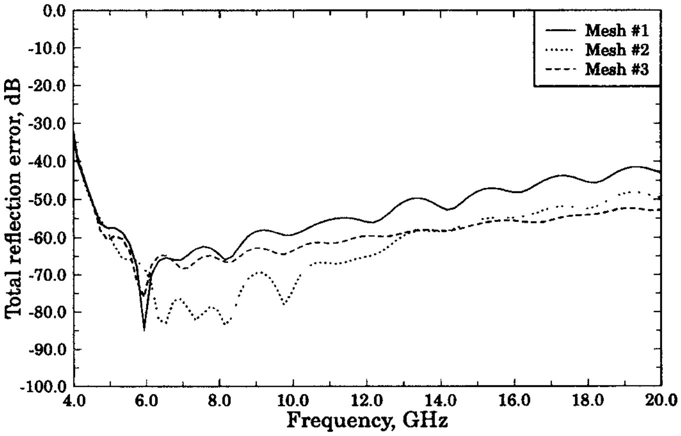

Fig. 3. Reflection error due to the PML termination for various finite element discretizations—$N = 10$, $d = 20$ mm, $m = 2$, $R = 1.0E - 4$, TM_1 mode.

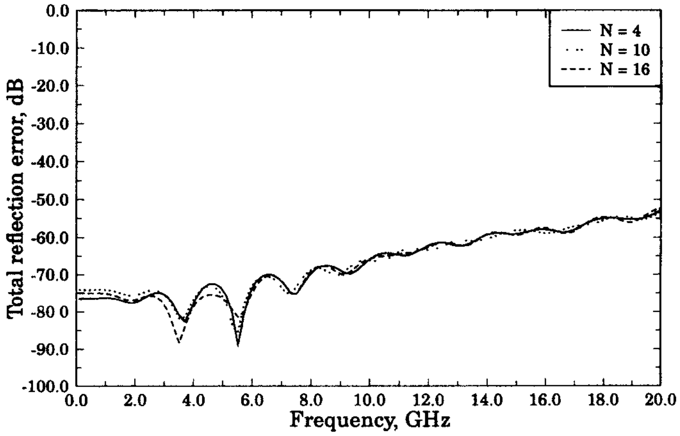

Fig. 5. The effect of increasing the number of layers, N, while keeping the depth of the PML region constant—Mesh #3, $m = 2$, $d = 20$ mm, $R = 1.0E - 4$, TEM mode.

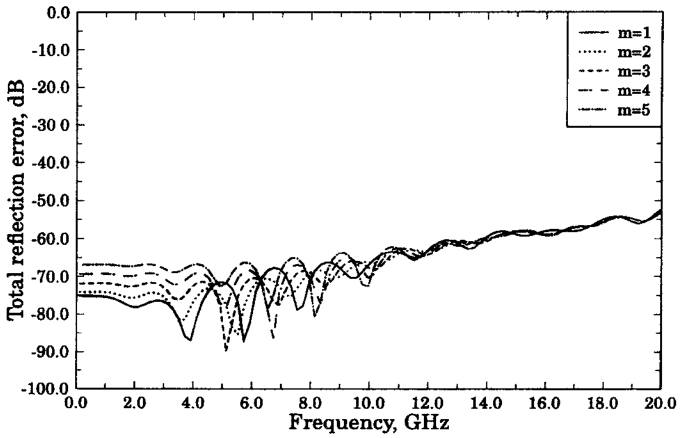

Fig. 4. The effect of the spatial polynomial order on the reflection error due to the PML termination—Mesh #3, $N = 10$, $d = 20$ mm, $R = 1.0E - 4$, TEM mode.

the reflection coefficient increases in the lower frequency range, whereas at higher frequencies the finite discretization effect dominates. In other words, the variation in the reflection coefficient due to changing the order of the spatial polynomial becomes increasingly smaller than the discretization error as the frequency of operation approaches higher values.

Another case of parameterization is to change the number of layers comprising the PML medium while keeping the total depth of the PML region constant. Fig. 5 shows the reflection coefficient versus frequency for three different values of N. The results illustrate that increasing the number of layers from $N = 4$ to $N = 16$, while keeping all other parameters constant, does not have a significant effect on the reflection coefficient. Note that for all three cases shown in Fig. 5 the domain discretization was kept the same.

IV. Conclusion

The PML absorbing boundary condition was implemented in a 2-D finite element formulation to solve waveguide propagation problems over a wide frequency range. The PML medium was modeled as a uniaxial anisotropic lossy material. A reflection error as low as −75 dB, which at low frequencies is attributed primarily to the PML termination, was shown for both cases (TEM and TM_1 modes) of waveguide excitation. Further improvement of the perfectly matched layer can be achieved by investigating the variation of the reflection error versus frequency for various parameters such as the depth of the PML region, the number of layers, the spatial polynomial order, etc. Additional parameterization of the PML absorbing boundary condition needs to be conducted.

Acknowledgment

The authors would like to thank Dr. J. F. Harvey of the Electronics Division, Army Research Office, and Dr. J. W. Mink, formerly of ARO, for their interest and support of the project.

References

[1] J. P. Berenger, "A perfectly matched layer for the absorption of electromagnetic waves," *J. Comp. Phys.*, vol. 114, no. 2, pp. 185–200, Oct. 1994.

[2] W. V. Andrew, C. A. Balanis, and P. A. Tirkas, "A comparison of the Berenger perfectly matched layer and the Lindman higher order abcs for the fdtd method," *IEEE Microwave Guided Wave Lett.*, vol. 4, no. 6, pp. 192–194, 1995.

[3] D. S. Katz, E. T. Thiele, and A. Taflove, "Validation and extension to three dimensions of the Berenger pml absorbing boundary condition for fdtd meshes," *IEEE Microwave Guided Wave Lett.*, vol. 4, no. 3, pp. 268–270, Aug. 1994.

[4] C. E. Reuter, R. M. Joseph, E. T. Thiele, D. S. Katz, and A. Taflove, "Ultrawideband absorbing boundary condition for termination of waveguiding structures in FD-TD simulations," *IEEE Microwave Guided Wave Lett.*, vol. 4, no. 10, pp. 344–346, Oct. 1994.

[5] U. Pekel and R. Mittra, "An application of the perfectly matched layer (PML) concept to the finite element method frequency domain analysis of scattering problems," *IEEE Microwave Guided Wave Lett.*, vol. 5, no. 8, pp. 258–260, Aug. 1995.

[6] Z. S. Sacks, D. M. Kingsland, R. Lee, and J.-F. Lee, "A perfectly matched anisotropic absorber for use as an absorbing boundary condition," *IEEE Trans. Antennas Propagat.*, vol. 43, no. 12, pp. 1460–1463, Dec. 1995.

[7] A. Taflove, *Computational Electrodynamics: The Finite-Difference Time-Domain Method.* Boston, MA: Artech House, 1995.